MORPHOLOGY OF PA6-NANOCOMPOSITE FIBRES BY MEANS OF ESEM STUDY OF FRACTURE SURFACES

C. Ibanes[1], K. Masenelli-Varlot[1], A. Malchère[1], R. Séguéla[1], L. David[2] and G. Robert[3]

[1] Groupe d'Etudes de Métallurgie Physique et de Physique des Matériaux, UMR CNRS 5510 ; INSA de Lyon ; bâtiment B. Pascal ; 7, avenue J. Capelle ; 69621 Villeurbanne cedex ; France
[2] Laboratoire des Matériaux Polymères et des Biomatériaux, ISTIL, 69622 Villeurbanne, France
[3] Rhodia Recherches ; Centre de Recherches de Lyon ; 85, rue des Frères Perret ; BP 62 ; 69192 Saint-Fons cedex ; France

ABSTRACT

Study of neat and filled PA6 fibres fracture surfaces at various draw ratios was carried out with a controlled pressure SEM. For the first time, observation could be done directly on fracture surface without metal coating. In order to ensure both negligible plastic deformations and a good reproducibility, a technique of sample preparation in liquid nitrogen was developed. Drawing brings molecular orientation, and modifies fracture morphology. The breakdown of as-spun fibres is brittle. Break morphology is transverse to the filament axis with a minimal smooth surface developed. As far as drawn fibres are concerned, fracture morphologies are either transverse "fibrous" break, or break with a tail and ridge or break by axial splitting. Surfaces developed during fracture are higher. Moreover, the fibrillar structure was revealed by the presence of fibrils, stacks of microfibrils of few tens nanometers in diameter. Skin / core structures were clearly highlighted. Fillers modifies little the fracture morphology of as spun filaments. In case of drawn fibres, the transverse mode seems promoted for polyamide fibres filled with organic highly-branched molecules. Break morphology with significant slip surfaces are observed in polyamide filled with montmorillonite drawn fibres, with longitudinal cracks. These two break morphologies are in agreement with the nature of fillers matrix interactions.

1. INTRODUCTION

Mechanical properties of semi-crystalline polymers sensitively depend on their microstructure, which can be controlled by stress, thermal and other parameters characteristic of the processes used to elaborate and process semi-crystalline polymers. These relations between the morphology and the macroscopic properties are particularly important in semi-crystalline fibres, where structural changes lead to significant differences in their mechanical properties. The fibre structure formation depends on condition of melt spinning and drawing: drawing increases stress at break and modulus, while the strain at break decreases [1].
Semi-crystalline polymer fibres have intricated structures. As far as nylon fibres are concerned, whose crystallinity index is generally lower than that of polyolefins, a description of a fibre structure was given in the literature [2]. According to this discription, a fibre is generally composed of dense microfibrils dispersed in a amorphous matrix (interfibrillar phase), composed of more or less oriented chains and tie-molecules between adjacent microfibrils. The microfibrils consist of amorphous and crystalline domains. Microfibrils are generally stacks of smaller fibrils, which diameters range between a few tens of nanometers to a few hundred of nanometers.

Although the mechanical properties of semi-crystalline polymers are sufficient around ambient temperature, they drop sensitively when the temperature reaches the glass transition temperature. The introduction of fillers is required to obtain a composite material with improved properties. From a general point of view, the maximum improvement of their mechanical properties should be observed with nano-sized fillers exhibiting a high aspect ratio. Mineral fillers with particles of nanometric size, i.e. nano-fillers, are well-known to bring an efficient mechanical reinforcement in semi-crystalline polymers above the glass transition temperature [3, 4], mainly due to their very high specific surface which provides an

extremely great number of polymer-filler and filler-filler interactions than conventional micrometric fillers. In the case of lamellar fillers such as montmorillonite, the large aspect ratio of the particles is also likely to promote a mechanical percolation of the filler particles at relatively low filler content. If much work has been carried out about the reinforcement of bulk thermoplastics by nano-fillers, very few studies have been reported in the case of fibres [5, 6]. Organic bulky dendrimers or hyperbranched (HB) macromolecules can also be considered as nano-fillers. Their specific properties rely on their three-dimensional structure and the great number of terminal functions. Such multifunctional globular macromolecules have been notably used as a dispersed minor component to improve processing and mechanical properties of thermoplastic blends [7, 8].

The understanding of structure – properties relationships of polymer fibres is of great scientific and technological importance. The fibre structure is generally studied by X-ray techniques [9, 10, 11]. Local Scanning Electron Microscopy observations of peel fibre or break surfaces were also carried out on polymeric fibres [12]. Textile fibre fractography was initially developed by Hearle [13, 14]. He established a classification of the main feature of fibre fracture morphologies obtained by tensile tests at various strain rates, or by fatigue tests. The three dimensional images clearly showed surface features, finish applications, wear and the nature and cause of fibre failure. Scanning Electron Microscopy has proven to be a very useful technique for the assessment of fibre morphology, such as molecular orientation, filament shape, diameter, assemblage of filaments, uniformity and surface structure. However, observations were possible only after metal coating, and on monofilaments with higher diameters to avoid sample charging under the electron beam [11, 12, 13].
It must be noted that study of polymer fibres would be incomplete if electron microscopy was the only technique applied. For example, Gupta and co. [15] studied the structure of aliphatic polyketones fibres by means of various complementary techniques such as X-ray diffraction, thermal analysis, tensile testing and electron microscopy. Therefore, our work can be included in a more complete study of the structure of neat and nano-filled polyamide 6 fibres at various draw ratio. The techniques used in the more complete study are small and wide angle X-ray scattering and a characterisation of the mechanical properties of the fibres [16].

In the current work, we examine the fracture behaviour of filled and unfilled polyamide fibres at various draw ratio, in order to gain some understanding on the reinforcement mechanisms. Our observations were carried out in a Environmental Scanning Electron Microscope (ESEM). Basically working like a conventional Scanning Electron Microscope, the main advantage of the ESEM for the characterisation of polymers is that, due to the presence of gas molecules in the chamber, samples do not need to be metal-coated. The technique has successfully been used to characterised natural fibres or polymers filled with spherical particles, which diameters lie in the range of about 200 nm [17, 18, 19]. Another way to avoid metal coating of polymeric surfaces is to work with a conventional SEM at low accelerating voltages, typically 1 keV [20]. This is possible only with a SEM is equipped with a Field Emission Gun, whose characteristic allows a good signal to noise ratio even at low accelerating voltages and at high magnifications. We found that images of the fibres' fracture surfaces were of better quality when using the ESEM under vacuum and at low accelerating voltage (typically 800 V) rather than under a partial pressure of H2O, mainly because nylon is highly H2O-sensitive (swelling effect).

Moreover, Energy-Dispersive Spectroscopy (EDS) in the SEM is a very efficient tool to detect the elements present and map their distributions in bulk materials. As far as polymers filled with inorganic nano-fillers are concerned, EDS can bring precious information regarding the dispersion of the filler. From a practical point of view, it is possible to detect an element only if the accelerating voltage is about 2.5 times the energy of the peak

characteristic of the element. Thus, in a conventional SEM working at low accelerating voltage, it is impossible to detect elements with atomic numbers higher than that of carbon ; mapping the distribution of aluminosilicates is utopian. On the contrary, the controlled pressure option of the ESEM offers the possibility of chemically analyse the specimen, which was not possible under vacuum because of the low acceleration voltage. The gas in the chamber indeed induces strong charge reduction of non-conducting specimens when exposed to the electron beam; observation of the specimen can thus be obtained at higher acceleration voltages. Simultaneous chemical analysis of the sample by EDS makes the ESEM well suited for the analysis of filled materials by observing the fracture surface and detecting the presence of chemical defects such as aggregates or agglomerates.

2. EXPERIMENTAL SECTION

The PA6 matrix had a weight-average molar weight Mw»80kDa. The highly-branched (HB) molecules were synthesised by polycondensation from di- and trifunctional monomers with COOH or NH2 end groups [21]. HB molecules consist of both aromatic and aliphatic segments, and have amine-terminated branches. Their weight-average molar weight was about 15kDa, their density was of the order of 1.25 g.cm-3. Thus, the diameter of HB molecules could be estimated to about 3.4 nm. The montmorillonite-based (MMT) fillers were composed of montmorillonite modified by a quaternary alkyl-ammonium surfactant, in order to ensure its exfoliation during processing. Both types of fillers were melt-compounded with the PA6 matrix using a twin-screw extruder prior to spinning: the 2HB-PA6, 5HB-PA6 and MMT-PA6 compounds contained 2 and 5 wt.% of HB and 1 wt.% of MMT, respectively.

Filaments of about 30 mm diameter were melt spun at 260°C, using a winding speed of 800 m/min. Bundles of 10 filaments were winded up together to form the so-called fibres that will be used in the study. The same spinning conditions were used for producing three kinds of filaments, i.e. PA6, HB-PA6 and MMT-PA6. Textile fibres generally have a surface finish applied following spinning, generally made of silicone oil, to aid handling of the fibres. The so-called fibres were drawn at a temperature of 140°C, at various draw ratios, λ: this latter is given by the ratio of the sample length after drawing to that prior to drawing.

Fibres were broken under flexural stress in liquid nitrogen. The two parts obtained were placed vertically on a SEM aluminium mount drilled with 1mm holes. Good electric and mechanical contact was ensured by silver glu. Samples were not metal-coated and were directly observed. Scanning electron micrographs of fracture surfaces using secondary electrons were acquired using a FEI ESEM XL-30 microscope in high vacuum mode and at very low tension (800V). The dispersion of fillers was studied by Energy Dispersive X-Ray Spectrometry (EDS), at 8 keV and under a controlled pressure of H-He (p=8 Torr).
Unfortunately, only a few images will be presented; the selected images point out important aspects of the fracture mechanisms. However, our discussion will be based on the failure characteristics of all the fibres broken. Reproducibility tests were carried out to ensure that the break morphologies observed were characteristic of the materials and did not depend on the preparation method. They were performed on at least 5 independently prepared fibres, each fibre being composed of 10 filaments.

2. RESULTS & DISCUSSION

Unfilled PA6 as spun fibres

Characteristic fracture surfaces for as spun PA6 fibres are reproduced in Figure 1. The diameter of each filament is measure to be about 28µm. The surfaces of the filament are rather smooth and no significant defect can be detected.

The main feature of as spun fibres fracture morphology is transverse crack propagation. As shown on Figure 1, all the 8 filaments of the same fibre present brittle fracture, at the same position in the fibre. The fracture surface are relatively smooth. After fracture, filaments remain stuck by 2 or 3. Yet, none of the PA6 as spun filaments were observed to be melted to another after spinning. Thus, this unambiguously shows that the surface finish still ensures the cohesion of the filaments. After initiation, the fracture may have propagated from one filament to the adjacent one due to the cohesion brought by the surface finish. The two ends of the same filament are strictly complementary, like mirror images (not shown). There is no production of debris. Besides, there is no evidence of crack initiation and propagation.

Several flats were created on the surfaces of the filaments, possibly due to the forced cohesion between the filaments after spinning and before crystallisation. Theses flats ensure a better cohesion of the fibre by enlarging the contact area. They might play a significant role in filament fracture, as crack initiator for example. This could explain why no crack initiation could be observed on the surfaces of the filaments, even when all the ten filaments of the same fibre could be observed.

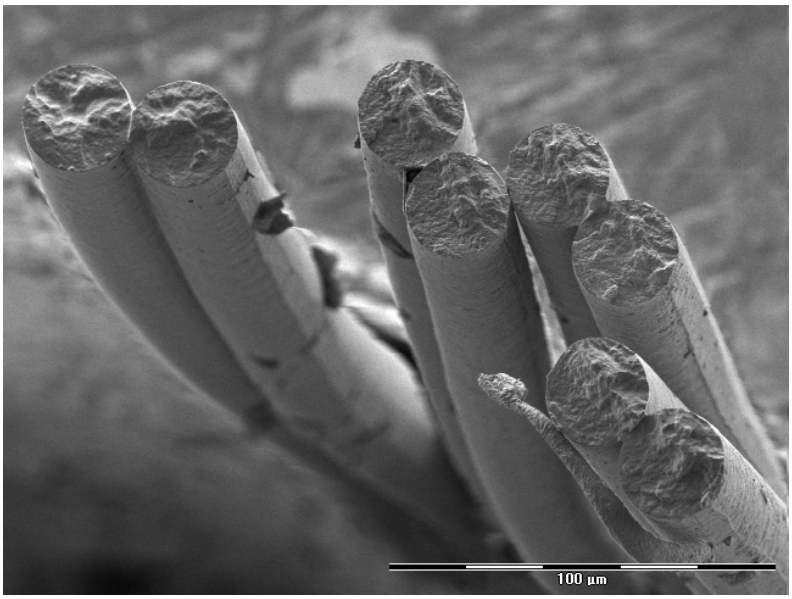

Fig. 1. Brittle failure of 8 as spun PA6 (λ=1) filaments. Scale bar : 100 mm.

Unfilled PA6 drawn fibres

WAXD spectra (not shown) show that upon drawing, the chain-twisted γ-phase gradually turns into the chain-extended α-phase. This γ to α strain-induced change was already reported in the case of fibres [22, 23, 24] and films [25, 26]. The gradual γ to α transformation upon drawing ends up into only a form at the maximum draw ratio. Moreover, the WAXS patterns of unfilled PA6 drawn fibres (not displayed) show that the a crystals become highly oriented, the chains being oriented parallel to the fibre axis.

Characteristic fracture surfaces for PA6 fibres at various draw ratios are reproduced on figure 2. There is a diameter dependence of the draw ratio: the average diameter for as spun PA6 filament is 28 ± 1 µm, the diameter equals 20 ± 1 µm for a draw ratio λ = 2.3 and is finally estimated to be 18 ± 1 µm for PA6 - λ = 2.65 filaments. The relation considering drawing

with constant volume which lies the diameter D and the draw ratio λ : $D \propto \lambda^{-0.5}$ is checked. Moreover, for highly drawn fibres, the filament surface is streak as shown on figures 7 and 9.

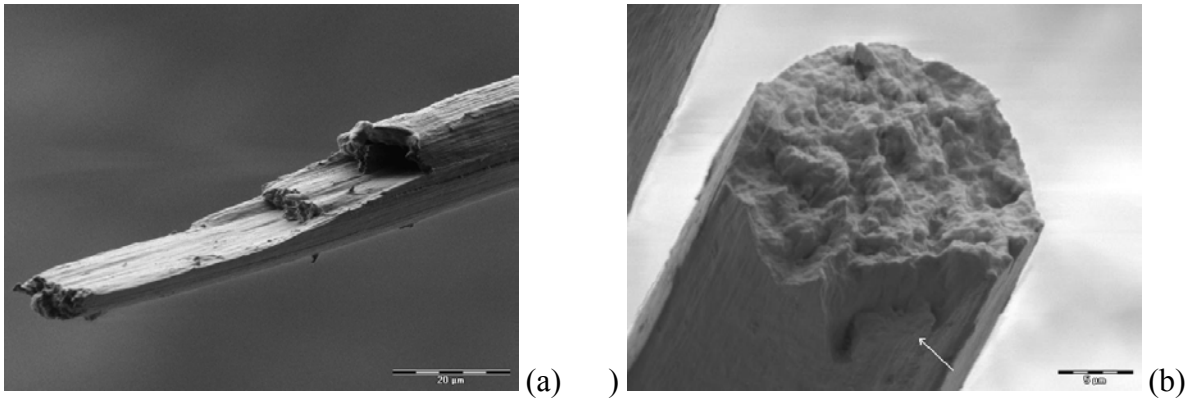

Fig. 2. (a) longitudinal break of a PA6 - λ=2.65 filament (scale bar : 10 mm) ; (b) transverse break of a PA6 - λ=2.3 filament (scale bar : 5 mm)

The observations reveal a fibrillar morphology that becomes more apparent with increasing draw ratio. The cohesion between the 10 filaments is generally destroyed by drawing. Drawn fibres break morphologies are various and might be classified as axial splitting (not displayed), transverse "fibrous" break (figure 2b) or longitudinal break with a tail and ridge.(figure 2a).

Transverse fracture surfaces of drawn fibres are characterised by an oriented fibrillar structure, with typical sizes ranging from 300 to 700 nm. Fine structure of drawn PA6 filaments indeed reveals the presence of several fibrils which diameters are close to about 50 nm (see figure 3). These fibrils are stacks of microfibrils. Fibrils are usually oriented in the same direction of drawing, which is not the case on the break morphology displayed on figure 3. We assume that the fibrils were actually oriented parallel to the fibre axis before breakdown, and collapsed on the surface after breakdown.

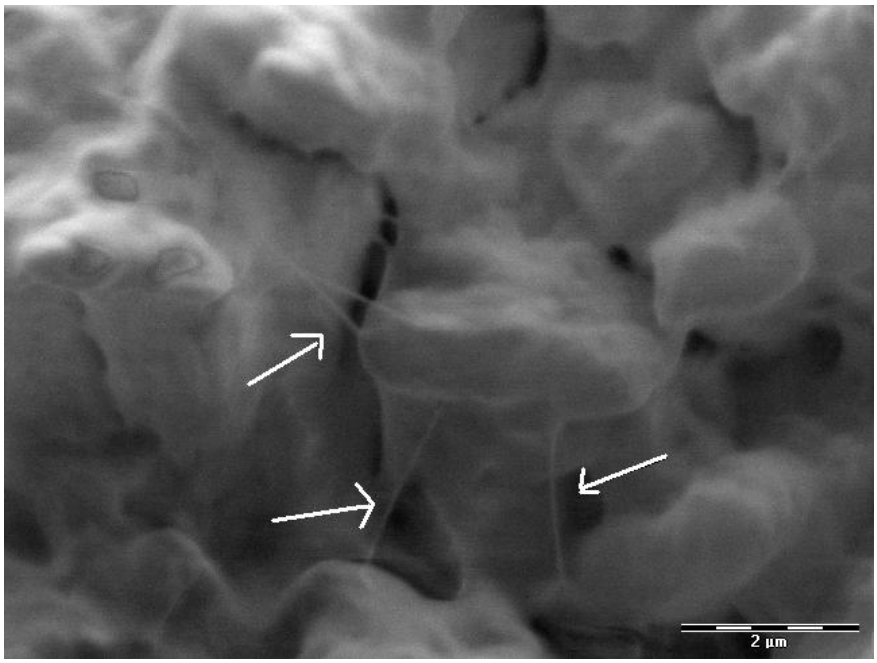

Fig. 3. Fibrillar microstructure of a PA6 - λ=2 filament, fine fibrils about 50nm in diameter. Scale bar : 2 mm.

The observation of antagonist parts of the same filament show that there is no fragment formation during fracture. The break morphology indicates that this is a “step by step” break. The crack is propagates along the microfibrils parallel to the drawing axis. When increasing drawing, the nature of the fracture tends toward a tail and ridge type fracture. It appears that the fracture may initiate at a defect near the surface, propagates along the microfibril boundaries and gradually works its way along and across the fibre to produce this characteristic failure appearance, as shown on figure 2a.

A skin-core structure was revealed, as displayed on figure 2b for a PA6 - λ=2.3 fibre. This skin-core morphology could not be clearly evidenced by X-ray scattering techniques, because X-Ray analyses are related to global information, on several fibres. The skin thickness is not uniform but it could be estimated to lie between 1 and 3 μm. This skin does not appear so clearly in as spun fibres, even though there is a gradual structure between the skin and the core. By drawing, this skin - core effect is expected to be amplified. Yet, the skin/core effect appears less clearly in highly drawn fibres (λ=2.65) compared to other less drawn fibres (λl=2.3). Indication of the skin/core effect is given by the presence of skin debris, as we can see on some of the filaments. Furthermore, this suggests that cracks propagate between the skin and the core of the filaments.

Filled fibres

As spun filled fibres are shown on figure 4. The break morphologies of as spun 2HB-PA6 are very similar to those of as spun 5HB-PA6 and are thus not displayed. The estimated diameters are 30 μm for the 2HB-PA6 and 5HB-PA6 and 31 μm for the MMT-PA6 filaments. The break morphologies are always brittle, without any fragment formation during fracture. The appearance of the fracture surfaces does not seem be modified by the presence of fillers. As for the neat as spun PA6 fibres, there is no evidence of crack initiation and propagation. EDS analyses of a MMT-PA6 filament (not displayed) indeed reveal uniform distributions of silicon and aluminium, which shows that there are no montmorillonite aggregates which could explain the crack initiation.

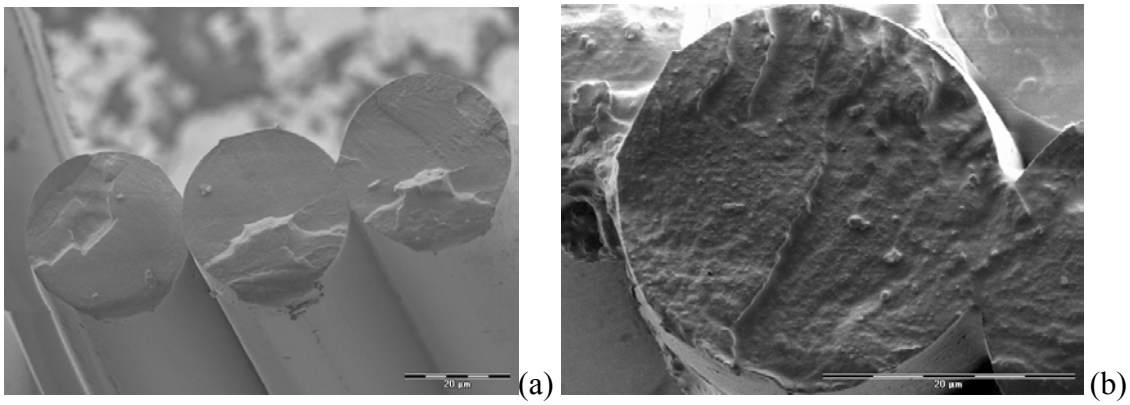

(a) (b)

Fig. 4. Brittle fracture of (a) 3 as spun HB-PA6 filaments filled with 5% HB (scale bar : 20 mm), and (b) one as spun MMT-PA6 filament (scale bar : 20 mm).

After initiation, the fracture most probably propagates into the adjacent filament due to the cohesion brought by the surface finish. After fracture, filaments remain stuck by 2 or 3 like in neat PA6 filaments. For example on figure 4b, two flats are visible on the transverse break surfaces of the as spun PA6-MMT filament. This filament seems to be welded with the filament on its right.

The diameters of drawn 2HB-PA6 fibres (λ=2.24) are estimated to range between 20.5 and 21.5 µm. Breaks for highly drawn PA6-HB fibres were frequently characterised as transverse "fibrous" breaks, as shown on figure 5a. The cohesion between fibrils seems to be increased by the organic fillers. This could explain that transverse "fibrous" breaks are the most commonly observed break morphologies. However, a mixed transverse and longitudinal break could sometimes be observed: Observation of highly drawn (λ=2.26) 5HB-PA6 filaments (not displayed) reveal a mixed transverse and longitudinal break morphology.

The part of transverse rupture shows a surface less oriented as compared with neat PA6 fibres at the same draw ratio. A crack in the middle of filament propagated longitudinally. This crack is connected with the transverse part of filament break by fine fibrils, which make bridges between the two sides of the crack. Organic fillers, due to their diameter of few nanometers, are supposed to reinforce the interfibrillar amorphous phase. HB molecules indeed have favourable interactions with the PA6 matrix. Amine terminated branches can set up a physical cross-link with PA6 chains through H-bonds, which increase the fibrillar cohesion. This could explain that most of the rupture morphologies of drawn HB-PA6 fibres can be classified as transverse "fibrous" breaks, yet with a less oriented structure than neat PA6 fibres at the same draw ratio.

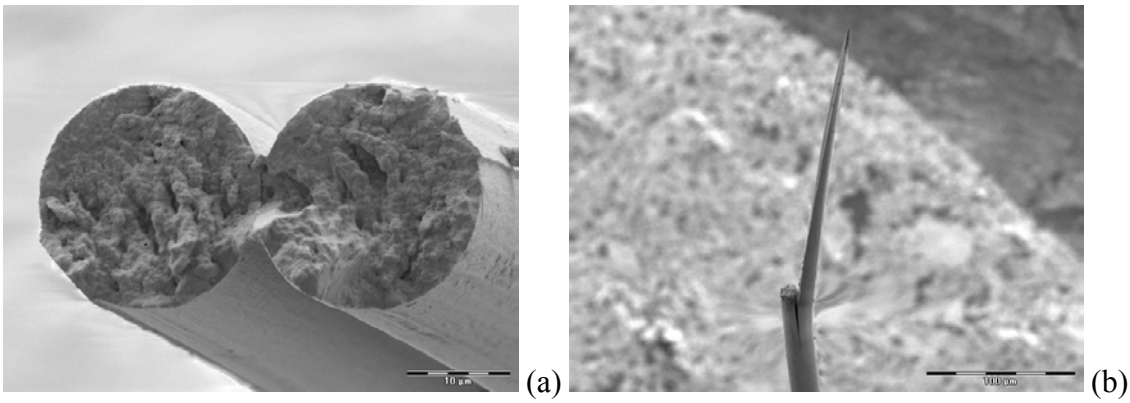

Fig. 5. (a) Transverse breaks of 2 drawn 2HB-PA6 filaments (λ=2.24). Scale bar : 10 mm. (b) drawn MMT-PA6 filament (λ=3.05) exhibiting a very long tail (scale bar : 100 mm).

Breaks for highly drawn MMT-PA6 fibres were frequently characterised by propagation of a crack, almost parallel to the direction of the fibres axis, as shown in figures 5(b). on this particular filament, the tail is about 175 nm long. The crack propagated along the fibre axis, also in the opposite direction. The surface developed during breakdown is very significant. The inner surface of the tail is very smooth, suggesting that there was an important slip. The inner surface of the tail also shows a fibrillar structure. Thus, the presence of MMT platelets most probably has lead to a loss of interfibrillar cohesion. Failure thus probably occurs because of a non-homogeneous inter-fibrillar cohesion. A break may then be produced and can be characterised by multiple axial splitting over a long length, equal to many fibre diameters.

The estimated diameters of λ=3.05 MMT-PA6 filaments lie between about 19 and 20 µm. The diameters of these highly drawn fibres do not check the relation between the diameter and the draw ratio. This indicate that the fibres do not undergo drawing with a constant volume. This may be an indication that voids are created in the fibres during drawing. The presence of elongated voids located between the microfibrils could be evidenced elsewhere by Small Angle X-Ray Scattering techniques [16]. Decohesion in the inter-fibrillar region may also be

promoted by the presence of elongated voids located between the microfibrils. The fracture morphology can also be partly explained by the extremely high surface to volume ratio of clay minerals and presumably weak polymer chain linkage to the mineral.

3. CONCLUSIONS

Our observations bring significant information on the structure of PA6 filled or unfilled fibres. Assemblage of filaments in fibres is essential, and makes it possible to understand the role of treatment surface and flats on the filament behaviour. In the case of as spun fibres, cohesion between the 10 filaments is very good. All filaments present brittle fractures only. The rupture propagates for one filament to another, probably through the flat parts of their surfaces. The break morphologies are always transverse. There are no evidence of crack initiation and propagation.

As far as drawn fibres are concerned, break morphologies are various. The flat part may induce break initiation. All the filaments show a fibrillar structure. When the rupture is transverse, the surface is very rough or "fibrous", as described by Hearle [11, 12]. On the other hand, when the rupture is longitudinal with a crack, surfaces parallel to the fibre axis are smoother or little grooved. Molecular orientation, i.e. fibrillar structures were observed in drawn fibres. Presence of fibrils is obvious; their diameters range between a few ten nanometers and a few thousand nanometers. This is in agreement with SAXS experiments [12].

Skin – core effects could be observed in drawn fibres. In most cases, this effect could not be clearly evidenced by X-ray scattering techniques, because X-Ray analyses give global information on several fibres. This skin – core structure plays a major role in the behaviour of drawn fibres: crack seems to initiate at the interface between the core and the skin of the fibres, as evidenced by the presence of some pieces of skin as debris.

Observations on filled fibres fracture surfaces bring some information on the reinforcement mechanisms. Organic fillers, due to their diameter of few nanometers, are supposed to reinforce the interfibrillar amorphous phase. HB molecules indeed have favourable interactions with the PA6 matrix. Amine terminated branches can set up a physical cross-link with PA6 chains through H-bonds, which increase the fibrillar cohesion. This could explain that most of the rupture morphologies of drawn HB-PA6 fibres can be classified as transverse "fibrous" breaks, yet with a less oriented structure than neat PA6 fibres at the same draw ratio.

In highly drawn MMT-PA6 fibres, failure occurs by cracking or splitting along planes close to the fibre axis. Due to a non-homogeneous inter-fibrillar cohesion, a break is produced and can be characterised by multiple axial splitting over a long length, equal to many fibre diameters. This process may also be promoted by the presence of elongated voids located between the microfibrils. Evidence for these voids include density decreases due to drawing and equatorial diffuse scattering observed in SAXS patterns [16]. The fracture morphology can also be partly explained by the extremely high surface to volume ratio of clay minerals and presumably weak polymer chain linkage to the mineral.

ACKNOWLEDGEMENTS

The authors would like to thank the Consortium Lyonnais de Microscopie Electronique (ClyME) for accessing the FEI ESEM XL-30 microscope and the Région Rhône-Alpes for its financial support.

References

1. **Gianchandani J., Spruiell J.E., Clark E.S.,** *J. Appl. Polym. Sci.* **27** (1982) 3527.
2. **Prevorsek D.C., Harget P.J., Sharma R.K., et al.,** *J.Macromol. Sci.-Phys.* **8/1-2** (1973) 127.
3. **Kojima Y., Usuki A., Kawasumi M., et al.,** *J. Mater. Res.* **8** (1993) 1185.
4. **Gloaguen J.M., Lefebvre J.M.,** *Polymer* **42** (2001) 5841.
5. **Giza E., Ito H., Kikutani T., et al.,** *J. Macromol. Sci.-Phys.* **B39** (2000) 545.
6. **Ergungor Z., Cakmak M., Batur C.,** *Macromol. Symp.* **185** (2002) 259.
7. **Fong H., Liu W., Wang C.H., Vaia R.H.,** *Polymer* **43** (2002) 775.
8. **Massa D.J., Shriner K.A., Turner S.R., Voit B.I.,** *Macromolecules* **28** (1995) 3214.
9. **Murthy N.S., Bednarczyk C., Moore R.A.F., et al.,** *J. Polym. Sci., Polym. Phys.* **34** (1996) 821.
10. **Samon J.M., Schultz J.M., Wu J., et al.,** *J. Polym. Sci., Polym. Sci.* **37** (1999) 1277.
11. **Samon J.M., Schultz J.M., Hsiao B.S.,** *Polymer* **41** (2000) 2169.
12. **Sawyer L.C., Grubb D.T.,** "*Polymer Microscopy"*. C. a. Hall, Ed. (Chapman and Hall, 1987).
13. **Hearle J.W.S., Cross P.M.,** *J. Mat. Sci.* **5** (1970) 507.
14. **Hearle J.W.S., Simmens S.C.,** *Polymer* **14** (1973) 273.
15. **Gupta P., Schulte J.T., Flood J.E., et al.,** *J. Appl. Polym. Sci.* **82** (2001) 1794.
16. **Ibanes C.,** "*Relations structure-propriétés mécaniques de fibres de polyamide 6 renforcées de nanoparticules organiques ou minérales"*, Ph-D thesis #03ISAL0052 (INSA de Lyon, Lyon, France, 2003).
17. **He C., Donald A.M.,** *J. Mater. Sci.* **32** (1997) 5661.
18. **Bos H.L., Donald A.M.,** *J. Mater. Sci.* **34** (1999) 3029.
19. **Stokes D.J.,** *Adv. Engin. Mater.* **3** (2001) 126.
20. **Kim G.M., Lee D.H.,** *J. Appl. Polym. Sci.* **82** (2001) 785.
21. Patent # WO 00/68298
22. **Samon J.M., Schultz J.M., Hsiao B.S.,** *Polymer* **41** (2000) 2169.
23. **Miyasaka K., Ishikawa K.,** *J. Polym. Sci., Polym. Phys.,* **6** (1968) 1317.
24. **Murthy N.S., Bray G.R., Correale S.T., Moore R.A.F.,** *Polymer* **36** (1995) 3863.
25. **Penel-Pierron L., Séguéla R., Lefebvre J.M., et al.,** *J. Polym. Sci., Polym. Phys.,* **39** (2001) 1224.
26. **Ito M., Takahashi A., Araki N., Kanamoto T.,** *Polymer* **42** (2001) 241.